

# Electrostatically Controlled Organization of Carboxylic Acid Derivatized Colloidal Silver Particles on Amine-Terminated Self-Assembled Monolayers

Anand Gole, S. R. Sainkar, and Murali Sastry\*

Materials Chemistry Division, National Chemical Laboratory, Pune-411 008, India

Received July 13, 1999. Revised Manuscript Received February 22, 2000

The formation of self-assembled monolayers (SAMs) of an aromatic bifunctional molecule, 4-aminothiophenol (4-ATP) on gold and the subsequent organization of carboxylic acid derivatized silver colloidal particles is described. Quartz crystal microgravimetry (QCM) measurements have been used to follow the formation of 4-ATP SAMs as well as electrostatic assembly of the colloidal silver particles on the SAM surface. It is shown that the electrostatic interaction between the negatively charged colloidal particle surface-bound carboxylic acid groups and the terminal amine groups in the SAM can be modulated by variation of the colloidal solution pH. This enables control over the surface coverage of the colloidal particles on the SAM surface with a maximum surface coverage of 18% being attained. The SAMs as well as the colloidal particle covered SAM films were further characterized with X-ray photoemission spectroscopy (XPS) and energy-dispersive analysis of X-rays (EDAX) measurements.

## Introduction

There is considerable current interest in the organization of colloidal nanoparticles in thin films. This is motivated to a large extent by the exciting physico-chemical and optoelectronic properties exhibited by nanoparticles, both individually<sup>1</sup> and collectively.<sup>2</sup> A number of strategies are being explored for assembling colloidal nanoparticles in 2-D. Some of the more extensively studied routes include self-assembly of colloidal nanoparticles via covalent interactions onto suitable substrates,<sup>3</sup> formation of films by the Langmuir–Blodgett technique<sup>4</sup> and by a simple solvent evaporation procedure.<sup>5</sup>

Electrostatic interactions, which play a crucial role in many chemical and biological processes,<sup>6</sup> have been used in the formation of multilayer films of cationic and

anionic colloidal silica and alumina particles<sup>7a</sup> and polyelectrolytes,<sup>7b,c</sup> in the immobilization of Keggin polyoxometalates at Langmuir monolayers,<sup>8</sup> in the complexation of proteins with lipid bilayers,<sup>9</sup> in the formation of nanoparticle–polyelectrolyte multilayers,<sup>10</sup> as well as in the self-assembly of micron sized objects.<sup>11</sup> In this laboratory, we have focused on using electrostatic interactions for the organization of surface-modified colloidal particles at the air–water interface<sup>12</sup> and via a diffusion process in fatty lipid thin films.<sup>13</sup> As part of

\* To whom correspondence should be addressed. Phone: +91-20-5893044. Fax: +91-20-5893952/5893044. E-mail: sastry@ems.ncl.res.in.

(1) (a) Klein, D. L.; Roth, R.; Lim, A. K. L.; Alivisatos, A. P.; McEuen, P. L. *Nature* **1997**, *389*, 699. (b) Ingram, R. S.; Hostetler, M. J.; Murray, R. W.; Schaff, T. G.; Khoury, J.; Whetten, R. L.; Bigioni, T. P.; Guthrie, D. K.; First, P. N. *J. Am. Chem. Soc.* **1997**, *119*, 9279.

(2) (a) Collier, C. P.; Saykally, R. J.; Shiang, J. J.; Henrichs, S. E.; Heath, J. R. *Science* **1997**, *277*, 1978. (b) Keating, C. D.; Kovaleski, K. K.; Natan, M. J. *J. Phys. Chem. B* **1998**, *102*, 9414.

(3) (a) Chumanov, G.; Sokolov, K.; Gregory, B. W.; Cotton, T. M. *J. Phys. Chem.* **1995**, *99*, 9466. (b) Colvin, V. L.; Goldstein, A. N.; Alivisatos, A. P. *J. Am. Chem. Soc.* **1992**, *114*, 5221. (c) Grabar, K. C.; Smith, P. C.; Musick, M. D.; Davis, J. A.; Walter, D. G.; Jackson, M. A.; Guthrie, A. P.; Natan, M. J. *J. Am. Chem. Soc.* **1996**, *118*, 1148. (d) Bandyopadhyay, K.; Patil, V.; Vijayamohan, K.; Sastry, M. *Langmuir* **1997**, *13*, 5244. (e) Garcia, M. E.; Baker, L. A.; Crooks, R. M. *Anal. Chem.* **1999**, *71*, 256. (f) Rizzo, R.; Fitzmaurice, D.; Hearn, S.; Hughes, G.; Spoto, G.; Ciliberto, E.; Kerp, H.; Schropp, R. *Chem. Mater.* **1997**, *9*, 2969.

(4) (a) Meldrum, F. C.; Kotov, N. A.; Fendler, J. H. *J. Phys. Chem.* **1994**, *98*, 4506. (b) Kotov, N. A.; Meldrum, F. C.; Wu, C.; Fendler, J. H. *J. Phys. Chem.* **1994**, *98*, 2735. (c) Sastry, M.; Patil, V.; Mayya, K. S.; Paranjape, D. V.; Singh, P.; Sainkar, S. R. *Thin Solid Films* **1998**, *324*, 239.

(5) (a) Brust, M.; Walker, M.; Bethell, D.; Schiffrin, D. J.; Whyman, R. *J. Chem. Soc., Chem. Commun.* **1994**, 801. (b) Brust, M.; Bethell, D.; Schiffrin, D. J.; Kiely, C. J. *Adv. Mater.* **1995**, *7*, 795. (c) Badia, A.; Gao, W.; Singh, S.; Demers, L.; Cuccia, L.; Reven, L. *Langmuir* **1996**, *12*, 1262. (d) Wang, Z. L.; Harfenist, S. A.; Whetten, R. L.; Bentley, J.; Evans, N. D. *J. Phys. Chem. B* **1998**, *102*, 3068. (e) Heath, J. R.; Knobler, C. M.; Leff, D. V. *J. Phys. Chem. B* **1997**, *101*, 189. (f) Wang, Z. L. *Adv. Mater.* **1998**, *10*, 13. (g) Connolly, S.; Fullam, S.; Korgel, B.; Fitzmaurice, D. *J. Am. Chem. Soc.* **1998**, *120*, 2969.

(6) Honig, B.; Nicholls, A. *Science* **1995**, *268*, 1144.

(7) (a) Iler, R. K. *J. Coll. Interface Sci.* **1966**, *21*, 569. (b) Taguchi, Y.; Kimura, R.; Azumi, R.; Tachibana, H.; Koshizaki, N.; Shimomura, M.; Momozawa, N.; Sakai, H.; Abe, M.; Matsumoto, M. *Langmuir* **1998**, *14*, 6550. (c) Lvov, Y.; Ariga, K.; Ichinose, I.; Kunitake, T. *J. Am. Chem. Soc.* **1995**, *117*, 6117.

(8) Clemente-Leon, M.; Agricole, B.; Mingotaud, C.; Gomez-Garcia, C. J.; Coronado, E.; Delhaes, P. *Langmuir* **1997**, *13*, 2340.

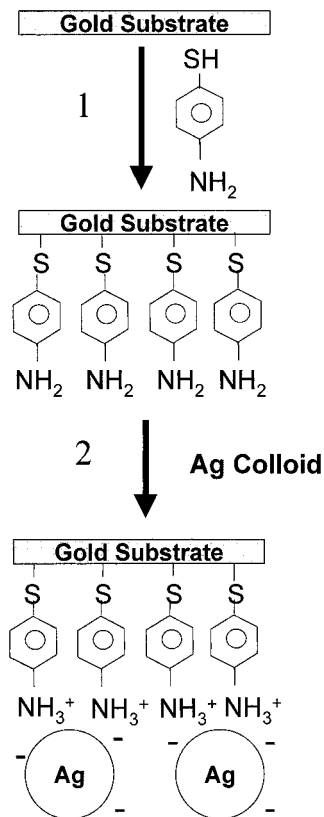
(9) Hamachi, I.; Fujita, A.; Kunitake, K. *J. Am. Chem. Soc.* **1994**, *116*, 8811.

(10) (a) Caruso, F.; Lichtenfeld, H.; Giersig, M.; Mohwald, H. *J. Am. Chem. Soc.* **1998**, *120*, 8523. (b) Lvov, Y.; Ariga, K.; Onda, M.; Ichinose, I.; Kunitake, T. *Langmuir* **1997**, *13*, 6195. (c) Sun, Y.; Hao, E.; Zhang, X.; Yang, B.; Shen, J.; Chi, L.; Fuchs, H. *Langmuir* **1997**, *13*, 5168.

(11) Tien, J.; Terfort, A.; Whitesides, G. M. *Langmuir* **1997**, *13*, 5349.

(12) (a) Mayya, K. S.; Patil, V.; Sastry, M. *Langmuir* **1997**, *13*, 2575. (b) Sastry, M.; Mayya, K. S.; Patil, V.; Paranjape, D. V.; Hegde, S. G. *J. Phys. Chem. B* **1997**, *101*, 4954. (c) Patil, V.; Mayya, K. S.; Pradhan, S. D.; Sastry, M. *J. Am. Chem. Soc.* **1997**, *119*, 9281. (d) Mayya, K. S.; Sastry, M. *J. Phys. Chem. B* **1997**, *101*, 9790. (e) Mayya, K. S.; Patil, V.; Sastry, M. *J. Chem. Soc., Faraday Trans.* **1997**, *93*, 3377. (f) Mayya, K. S.; Sastry, M. *Langmuir* **1998**, *14*, 74. (g) Mayya, K. S.; Patil, V.; Kumar, M.; Sastry, M. *Thin Solid Films* **1998**, *312*, 308. (h) Sastry, M.; Mayya, K. S.; Patil, V. *Langmuir* **1998**, *14*, 5198.

**Scheme 1. Diagram Showing the Various Stages of Formation of Silver Colloidal Particles on 4-ATP SAMs<sup>a</sup>**



<sup>a</sup> Step 1: SAM formation of 4-ATP. Step 2: Immersion of the 4-ATP SAM formed on gold in the 4-CTP-capped silver colloidal solution to electrostatically immobilize the silver clusters.

our ongoing efforts to use electrostatic interactions for the organization of nanoparticle assemblies, we have investigated the possibility of electrostatically immobilizing carboxylic acid derivatized colloidal silver nanoparticles on amine-terminated self-assembled monolayers (SAMs). We demonstrate herein that this can be achieved by a simple two-step process. The first step consists of formation of SAMs of a bifunctional molecule, 4-aminothiophenol (4-ATP), on gold (Scheme 1, step 1) while the 2-D assembly of the colloidal nanoparticle film is accomplished in the second step by simple immersion of the 4-ATP SAM covered substrate in the carboxylic acid derivatized silver colloidal solution (Scheme 1, step 2). An advantage of this approach is that the surface coverage of the silver nanoparticle film can be controlled by modulating the electrostatic interaction between the negatively charged silver particles and the positively charged amine-terminated SAM surface via variation of the colloidal solution pH. Furthermore, the silver colloidal particle monolayer electrostatically immobilized on the 4-ATP SAM may be desorbed (and thereafter, reversibly adsorbed on the 4-ATP SAM) by a similar variation of the colloidal solution pH thus highlighting an important advantage over colloidal

particle films formed by covalent attachment to surfaces. The formation of the silver nanoparticle films has been characterized using quartz crystal microgravimetry, X-ray photoelectron spectroscopy (XPS), and energy-dispersive analysis of X-ray (EDAX) measurements. Presented below are details of the investigation.

### Experimental Details

The silver colloidal particles were synthesized in aqueous medium by borohydride reduction of  $\text{Ag}_2\text{SO}_4$  solution as described elsewhere.<sup>12b,13a</sup> This procedure yields silver particles of  $70 \pm 13$  Å size in a hydrosol at a pH of  $\sim 9$ .<sup>12b</sup> The colloidal particles were thereafter capped with 4-carboxythiophenol (4-CTP) by addition of a solution of 4-CTP in absolute ethanol to yield an overall capping concentration of  $10^{-5}$  M in the hydrosol. The capping of the colloidal particles was followed by using UV-vis spectroscopy, which showed a shift and damping of the surface plasmon resonance from 388 nm for the uncapped sol to 398 nm on capping.<sup>12b</sup>

The kinetics of self-assembly of 4-ATP on gold was monitored using quartz crystal microgravimetry (QCM). This was done by following the change in the resonance frequency of a gold-coated AT-cut 6 MHz quartz crystal as a function of time of immersion in a  $10^{-3}$  M concentrated ethanolic solution of 4-ATP. The frequency of the quartz crystal was measured using an Edwards FTM5 frequency counter which had a stability and resolution of 1 Hz. This translates to a mass resolution of 12 ng/cm<sup>2</sup> for the 6 MHz crystal used. Frequency measurements were made ex-situ after thorough washing of the crystals in copious amounts of ethanol and drying in flowing  $\text{N}_2$ . The measured frequency changes were converted to mass loading of the crystal using the standard Sauerbrey equation.<sup>14</sup> In a control experiment, a methyl-terminated octadecanethiol (ODT) SAM as grown on a gold-coated QCM quartz crystal by immersion of the crystal in a  $10^{-3}$  M ethanolic solution of ODT for 3 h. 4-ATP SAMs were also grown on thermally evaporated gold films of 2000 Å thickness on Si (111) wafers and were used for additional XPS and EDAX analysis. The gold film deposition was carried out in an Edwards 306E thin film coating unit equipped with a liquid nitrogen trap. The deposition was carried out at a pressure of  $1 \times 10^{-7}$  Torr and was monitored using a quartz-crystal microbalance (QCM). After formation of a close-packed monolayer of 4-ATP, the gold-coated quartz crystals as well as the gold films on Si were further immersed in the 4-CTP-capped silver hydrosol maintained at different pH values in the range 6–11. The pH values were adjusted using dilute  $\text{H}_2\text{SO}_4$  and NaOH solution. As in the case of formation of 4-ATP SAMs, the mass loading of the QCM crystal during attachment of the silver clusters to the 4-ATP SAM surface was monitored ex-situ as a function of time after washing of the crystals with deionized water and drying in  $\text{N}_2$ . It is to be noted that for each immersion of the 4-ATP SAM covered QCM crystal in the silver colloidal solutions held at different pH, a fresh 4-ATP SAM was used. In a parallel control experiment, the ODT SAM grown on a QCM quartz crystal was immersed in the silver colloidal solution at pH = 9 and the mass change recorded ex-situ as a function of time. Measurements were also performed wherein a silver colloidal particle monolayer on the 4-ATP SAM grown on a QCM crystal at maximum coverage (formed at a colloidal solution pH = 9) was immersed in silver colloidal solutions maintained at different pH values in the range 6–11 for 90 min. Here again, a fresh 4-ATP SAM with maximum coverage of the silver clusters was used in each one of the immersion cycles. The desorption of the silver colloidal particles from the above substrates after immersion in the silver colloidal solutions at different pH was characterized in terms of the QCM mass loss recorded ex-situ as well as the atomic ratio of Ag:Au estimated using EDAX measurements on the same QCM quartz crystal. EDAX measurements were carried out on a Leica Stereoscan-

(13) (a) Sastry, M.; Patil, V.; Mayya, K. S. *Langmuir* **1997**, *13*, 4490. (b) Patil, V.; Sastry, M. *J. Chem. Soc. Faraday Trans.* **1997**, *93*, 4347. (c) Patil, V.; Sastry, M. *Langmuir* **1997**, *13*, 5511. (d) Sastry, M.; Patil, V.; Sainkar, S. R. *J. Phys. Chem. B.* **1998**, *102*, 1404. (e) Patil, V.; Sastry, M. *Langmuir* **1998**, *14*, 2707.

(14) Sauerbrey, G. *Z. Phys. (Munich)* **1959**, *155*, 206.

440 scanning electron microscope (SEM) equipped with a Phoenix EDAX attachment.

The SAM/silver colloidal particle assembly formed on gold-coated Si wafers under optimum pH conditions (i.e., maximum cluster adsorption) was investigated by X-ray photoemission spectroscopy (XPS). XPS measurements were carried out on a VG Scientific ESCA 3 MK II spectrometer at a pressure better than  $1 \times 10^{-9}$  Torr. The electrons were excited with unmonochromatized Mg K $\alpha$  X-rays (energy = 1253.6 eV) and the spectra were collected in the constant analyzer energy mode at a pass energy of 50 eV. This leads to an overall resolution of  $\sim 1$  eV for the measurements. Au 4f (substrate), Ag 3d, C 1s, N 1s, and S 2p spectra were recorded from the SAM/silver colloid film at an electron takeoff angle (angle between the surface plane and electron emission direction) of 75°. Prior to curve stripping by a nonlinear least squares procedure, the inelastic electron background was removed by the Shirley algorithm.<sup>15</sup>

Attempts were made to image the colloidal particle monolayer by atomic force microscopy (AFM) but failed due to instability of the colloidal particle monolayer during movement of the AFM tip over the surface. This may be a consequence of the relatively weak electrostatic bonds between the colloidal particles and the 4-ATP SAM as evidenced by QCM studies which indicated facile desorption of silver colloidal particles on modulation of the electrostatic interactions by solution pH variation (see Results and Discussion below).

## Results and Discussion

SAMs of 4-ATP both on gold and silver surfaces have been studied extensively in electrochemical applications,<sup>16</sup> as surface modifiers for stable, reactive liquid-phase acoustic wave sensor applications,<sup>17</sup> to chemically modify scanning tunneling microscopy tips,<sup>18</sup> and in the development of surface-plasmon resonant immunosensors.<sup>19</sup> As shown in the previous reports,<sup>16–19</sup> formation of thiolate linkages between the 4-ATP molecules and gold/silver leads to amine functionalization of the metal film surface (Scheme 1, step 1). Figure 1 shows the QCM mass uptake recorded as a function of time of immersion of the gold-coated AT-cut quartz crystal in a  $10^{-3}$  M concentrated ethanolic solution of 4-ATP. The frequency changes of the quartz crystal were measured ex-situ as noted in the Experimental Section. It can be seen from the figure that the mass uptake is initially rapid and complete monolayer formation occurs within  $\sim 70$  min of immersion. The solid line is an aid to the eye and has no physical significance. The equilibrium mass uptake was determined to be  $\sim 110$  ng/cm<sup>2</sup> and results in an area per 4-ATP molecule of  $\sim 19$  Å<sup>2</sup>, indicating fairly close-packing of the 4-ATP molecules.<sup>20</sup> We point out that the packing of 4-ATP SAMs is more dense than that of the 4-CTP SAMs (area per 4-CTP molecule of 25 Å<sup>2</sup>) of our earlier study.<sup>21</sup> This may be a consequence

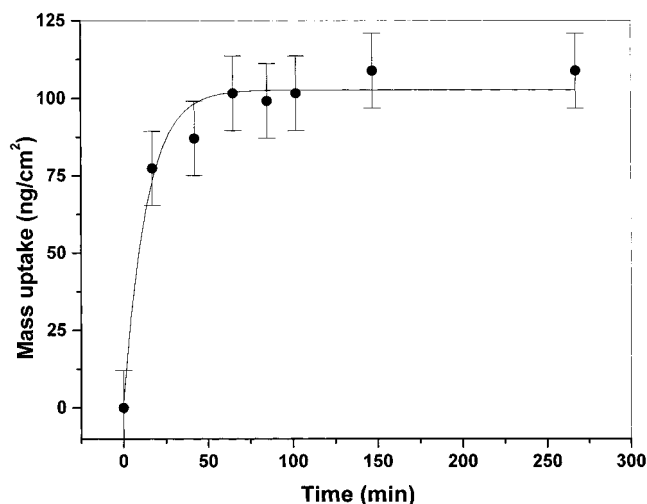


**Figure 1.** QCM mass uptake with time during formation of a 4-ATP SAM on a gold-coated AT-cut quartz crystal.

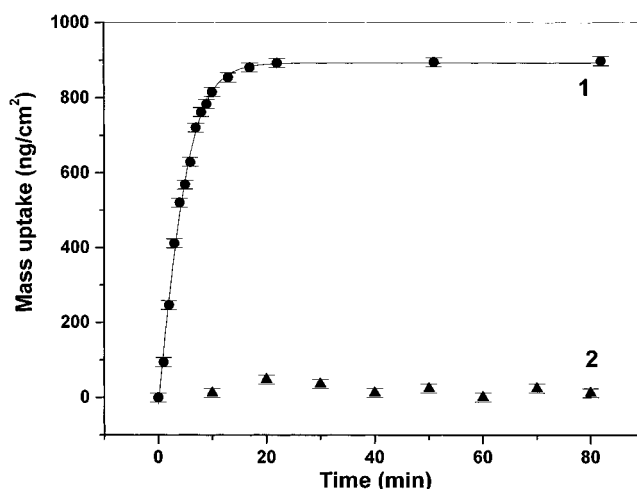


**Figure 2.** Curve 1: QCM mass uptake with time during electrostatic attachment of 4-CTP-capped silver colloidal particles on a 4-ATP SAM formed on gold (see Figure 1) at a colloidal solution pH = 9. Curve 2: QCM mass uptake recorded ex-situ with time of immersion of an ODT SAM grown on a gold-coated QCM crystal in the silver colloidal particle solution maintained at pH = 9.

of purely steric factors determined by the size of the terminal groups,<sup>20</sup> the amine group being less bulky than the carboxylic acid group. From this stage of the investigation, an optimum SAM formation time of 4 h was determined and used in the formation of 4-ATP SAMs on thermally evaporated gold films for the XPS measurements.

After steady-state surface coverage of the 4-ATP SAM on the gold-coated quartz crystal was achieved, the SAM was immersed in the carboxylic acid derivatized silver colloidal solution maintained at the as-prepared pH of 9 (Scheme 1, step 2). Figure 2 (curve 1) shows the QCM mass uptake measured ex-situ as a function of time during cluster attachment to the 4-ATP SAM as described in the Experimental Section. It is observed that the mass uptake is fairly rapid with the equilibrium colloidal particle coverage being achieved within 30 min of immersion. The equilibrium mass uptake of  $\sim 900$  ng/cm<sup>2</sup> corresponds to a surface coverage of  $\sim 18\%$  assuming electrostatic immobilization of 70 Å diameter silver

(15) Shirley, D. A. *Phys. Rev. B* **1972**, *5*, 4709.

(16) (a) Bryant, M. A.; Crooks, R. M. *Langmuir* **1993**, *9*, 385. (b) Hayes, W. A.; Shannon, C. *Langmuir* **1996**, *12*, 3688. (c) Liu, S. Q.; Tabg, Z. Y.; Bo, A. L.; Wang, E. K.; Dong, S. J. *J. Electroanal. Chem.* **1998**, *458*, 87. (d) Lukkittari, J.; Kleemola, K.; Mercetoja, M.; Kankare, J. *Langmuir* **1998**, *14*, 1705. (e) Rubinstein, I.; Rishpon, J.; Sabatani, E.; Redondo, A.; Gottesfeld, S. *J. Am. Chem. Soc.* **1990**, *112*, 6135.

(17) (a) Chance, J. J.; Purdy, W. C. *Thin Solid Films* **1998**, *335*, 237. (b) Rousha, J. A.; Thacker, D. L.; Anderson, M. R. *Langmuir* **1994**, *10*, 1642.

(18) Ito, T.; Buhlmann, P.; Umezawa, Y. *Anal. Chem.* **1998**, *70*, 255.

(19) Disley, D. M.; Cullen, D. C.; You, H. X.; Lowe, C. R. *Biosensors Bioelectronics* **1998**, *13*, 1213.

(20) Kim, Y. T.; McCarley, R. L.; Bard, A. J. *J. Phys. Chem.* **1992**, *96*, 7416.

(21) Sastry, M.; Patil, V.; Mayya, K. S. *J. Phys. Chem. B* **1997**, *101*, 1167.

clusters. This value agrees very well with the maximum effective packing density that we could achieve for electrostatically formed nanocomposites of colloidal particles and fatty lipids<sup>13a</sup> and is slightly less than the coverage of 30% reported for silver colloidal particles immobilized on surface modified polymer films.<sup>3c</sup> The repulsive electrostatic interactions between the colloidal particles apparently prevents higher packing densities of the colloidal particles from being achieved.<sup>3c</sup> The QCM mass changes measured for an ODT SAM on a gold-coated quartz substrate as a function of time of immersion in the silver colloidal solution are also shown in Figure 2 (curve 2). We point out here that the mass change recorded after formation of the ODT monolayer indicated close-packing of the hydrocarbon chains with an area of  $\sim 22 \text{ \AA}^2$  per ODT molecule. It is observed from Figure 2 (curve 2) that there is negligible cluster adsorption onto the ODT SAM surface, clearly indicating that the terminal amine group in the 4-ATP SAM is playing an important role in electrostatically immobilizing the 4-CTP-capped silver particles on the SAM surface.

In our earlier studies on the electrostatic assembly of carboxylic acid derivatized colloidal particles with fatty amine Langmuir monolayers<sup>12</sup> and thermally evaporated fatty amine films,<sup>13</sup> we had observed that the cluster density in the composite films could be controlled by varying the pH of the colloidal solution. A similar study was carried out using the 4-ATP SAMs of this investigation as well. 4-ATP SAMs grown on the gold-coated quartz crystals were immersed in the silver colloidal solutions maintained at different pH values in the range 6–11 for 5 h.<sup>22</sup> The mass uptake after this time of immersion was measured ex-situ after thorough washing of the crystals with deionized water and drying. Figure 3 shows the silver particle surface coverage in the above experiment plotted as a function of the silver colloidal solution pH. It can be seen that the colloidal particle surface coverage is a maximum at pH = 9 and falls to both higher and lower pH values. The data have been fit to a Lorentzian, the curve being shown as a solid line. The various regions in the electrostatic response curve may be explained with schemes as shown in the figure. At pH values lower than 8, the carboxylic acid groups on the colloidal particle surface become progressively less ionized (Figure 3, schematic at the left edge) while the amine groups are fully ionized. This reduces the electrostatic coupling between the colloidal particles and the ionized amine groups in the SAM and leads to a lower surface coverage of the adsorbed particles. At a pH value close to 9, both the amine groups of the SAM and the carboxylic acid groups of the silver particles are fully ionized, leading to maximum attractive electrostatic interaction and thus, the maximum possible particle surface coverage (Figure 3, schematic at the center). As the pH is increased above 9, the exposed amine groups of the SAM become progressively less ionized while the silver clusters are

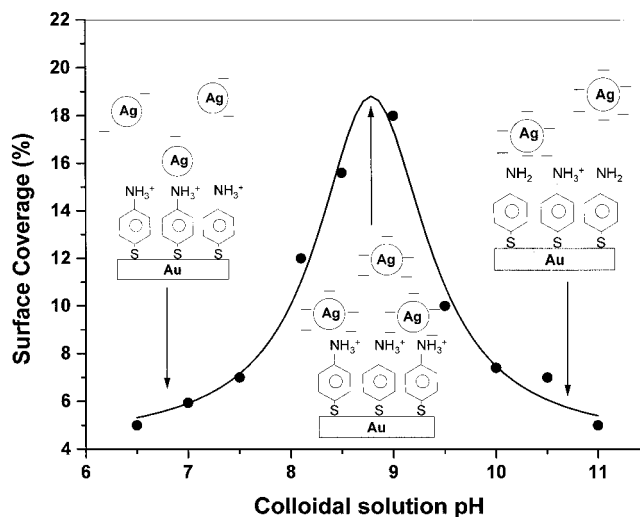


**Figure 3.** Surface coverage of 4-CTP-capped silver colloidal particles on 4-ATP SAMs plotted as a function of colloidal solution pH used for the formation of the colloidal particle films. The schematics show the nature of electrostatic coordination in the different pH regimes.

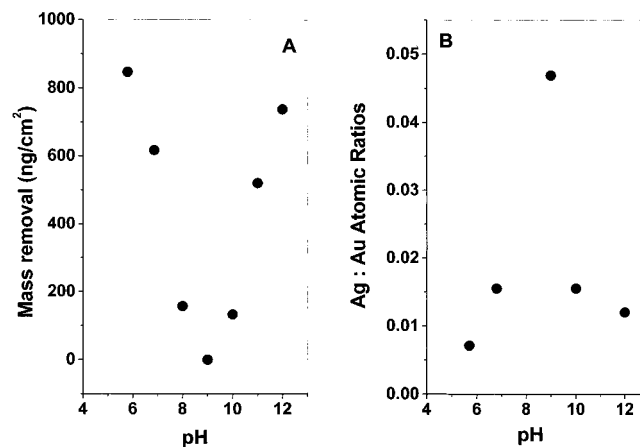


**Figure 4.** (A) QCM mass losses recorded ex-situ from silver colloidal particle films at maximum surface coverage after immersion in silver colloidal particle solutions maintained at different pH values. (B) EDAX Ag:Au atomic ratios measured for the silver colloidal particle films subjected to QCM investigation and shown in part A.

fully charged and lead consequently to a reduced surface coverage of the clusters (Figure 3, schematic at extreme right). The variation in surface coverage of the clusters with colloidal solution pH thus represents a sort of convolution of the individual titration curves of the amine groups in the SAM and the carboxylic acid groups immobilized on the surface of the silver particles.

Another important test of the electrostatic bond formation between the colloidal particle bound carboxylic acid groups and the amine terminal groups in the SAM would be the desorption of the silver colloidal particles from the SAM surface on immersion of the film in colloidal solutions at pH values where the electrostatic interactions are reduced. Figure 4A shows the QCM mass loss recorded ex-situ from silver colloidal particle films at maximum surface coverage (formed at pH = 9) after immersion in silver colloidal particle solutions at different pH values for 90 min. A parallel EDAX study was carried out on the same films used in

(22) The lower limit to the pH range was determined by the stability of the silver colloids. At pH values lower than 6, the carboxylic acid groups on the particle surface are progressively less ionized. The electrostatic stabilization of the hydrosol is thus removed leading to flocculation of the colloidal particles as shown in: (a) Sastry, M.; Bandyopadhyay, K.; Mayya, K. S. *Colloid Surf. A* **1997**, *127*, 221. (b) Mayya, K. S.; Patil, V.; Sastry, M. *Langmuir* **1997**, *13*, 3944.

the QCM measurements mentioned above, and the Ag:Au atomic ratios obtained as a function of colloidal solution pH are plotted in Figure 4B. As mentioned earlier, each data point in the figure represents a fresh silver colloidal particle film (formed under maximum surface coverage conditions) immersed in the silver sol at that particular pH. It can be seen from Figure 4A that there is a progressively increasing desorption of the silver colloidal particles from the monolayer into solution as the pH of the solution is decreased below 9 as well as above pH = 9. Figure 4B corroborates this finding and shows that the Ag:Au atomic ratio estimated from EDAX measurements decreases above and below pH = 9. The EDAX measurements also provide additional independent support to the variation in surface coverage of the silver colloidal particle monolayer formed on the 4-ATP SAM indicated by the QCM studies presented earlier (Figure 3). The pH-dependent desorption of the silver colloidal particles clearly indicates that electrostatic bonds between the carboxylic acid groups on the silver particle surface and amine groups in the 4-ATP SAM are responsible for immobilization of the silver particles on the SAM surface. This also highlights an important advantage of the electrostatic immobilization procedure for colloidal particles demonstrated in this paper over the covalent attachment procedure which is irreversible.

A comparison of the electrostatically controlled adsorption and desorption data obtained from QCM measurements and plotted in Figures 3 and 4A, respectively, indicates some differences in the equilibrium surface coverage of the silver colloidal particles during immersion in different pH silver solutions. For example, the surface coverage of silver clusters adsorbed on the 4-ATP SAM surface at pH = 10 is ~7% (Figure 3) while the surface coverage of silver clusters obtained by desorption of a fraction of the maximum coverage silver film by immersion in silver colloidal solution at pH = 10 is calculated to be 15%. This difference may be a consequence of the fact that the initial state of the 4-ATP monolayer in both cases is quite different, i.e., during the adsorption process, all the amine groups on the 4-ATP SAM surface are accessible to electrostatic interaction while in the desorption process, the initial state is one of SAM surface covered with colloidal silver particles at close to maximum packing. It is clear that in the latter case, the electrostatically modulated desorption process of the silver particles (via variation in the colloidal solution pH) will be influenced by the interaction between the already adsorbed silver particles themselves and could thus affect the final state equilibrium coverage of the silver particles. The adsorption/desorption process is thus dependent on the history of the sample and is path dependent.

The electrostatically organized monolayer of the silver colloidal particles on the 4-ATP SAM was investigated chemically using XPS, the cluster attachment being done at pH = 9 where maximum cluster adsorption occurs (see preceding discussion and Figure 3). The Au 4f (from the substrate), Ag 3d, C 1s, O 1s, N 1s, and S 2p core level spectra were recorded as mentioned in the Experimental Section. The signal-to-noise ratio for the S 2p and N 1s core level spectra was not good enough for carrying out an accurate chemical analysis and,

**Table 1. Parameters Obtained from Fits to the Core Level XPS Spectra Recorded from an Electrostatically Immobilized Ag Colloidal Particle Film on a 4-ATP SAM on Gold**

core level	BE 1 (eV)	BE 2 (eV)	BE 3 (eV)
Au 4f <sub>7/2</sub>	84.0		
Ag 3d <sub>5/2</sub>	368.7	370.6	
C 1s	286.5	288	290.3
O 1s	531.2	532.9	

therefore, will not be discussed further. The core level spectra mentioned above were decomposed into individual chemical components using a nonlinear least-squares fitting procedure (see Supporting Information, Figures 1–4), and the parameters obtained from the fits are listed in Table 1. The primary objective of the XPS studies was to provide a preliminary chemical analysis of the silver colloidal monolayer formed on the 4-ATP SAM to complement the QCM studies presented earlier. A detailed analysis of the colloidal particle film formed will be presented elsewhere after additional XPS measurements.

The Au 4f spectrum consists of a single spin-orbit component with the Au 4f<sub>7/2</sub> component at 84 eV taken as the binding energy (BE) reference level and all other spectra were shifted accordingly to determine the chemical shifts. The Ag 3d spectrum consists of two spin-orbit components with the Ag 3d<sub>5/2</sub> binding energies for the two components being 368.7 and 370.6 eV (Table 1). The low BE component may be assigned to metallic Ag<sup>23</sup> while the higher BE component is tentatively assigned to a sulfonate group coordinated to Ag,<sup>24</sup> which is expected to form a concentric shell around the metal core. The oxidation of the sulfur groups could occur on both 4-CTP and 4-ATP molecules and are indicated by the large BE of one of the components observed in the O 1s spectrum (to be discussed below). The C 1s spectrum was decomposed into three chemically distinct components at 286.5, 288, and 290.3 eV (Table 1). These components are assigned to the carbons in the aromatic rings of 4-ATP and 4-CTP, the carbon coordinated to the carboxylic acid group in 4-CTP and carbon coordinated to a sulfonate group respectively and agree well with those obtained in earlier studies on Langmuir–Blodgett films and SAMs containing similar functional groups.<sup>24,25</sup> The O 1s spectrum could be decomposed into two components with BEs at 531.2 and 532.9 eV. The low BE component is assigned to oxygen in the carboxylic acid groups of 4-CTP<sup>25b,c</sup> while the high BE component is tentatively associated with oxygen in a sulfonate moiety.<sup>24</sup> On the basis of analysis of the O 1s core level, it is possible that the high BE component in the Ag 3d spectrum could be due to coordination with the sulfonate moiety of 4-CTP as mentioned earlier.

In conclusion, it has been shown that amine-terminated SAMs of an aromatic molecule, 4-ATP, can be used to electrostatically immobilize carboxylic acid

(23) (a) Kaushik, V. K. *J. Electron Spectrosc.* **1991**, *56*, 273. (b) Gaarenstroom, S. W.; Winograd, N. *J. Chem. Phys.* **1987**, *67*, 3500.

(24) Bandyopadhyay, K.; Mayya, K. S.; Vijayamohan, K.; Sastry, M. *J. Electron Spectrosc.* **1997**, *87*, 101.

(25) (a) Ganguly, P.; Paranjape, D. V.; Sastry, M.; Chaudhari, S. K.; Patil, K. R. *Langmuir* **1993**, *9*, 487. (b) Sastry, M.; Ganguly, P. *J. Phys. Chem. A* **1998**, *102*, 697. (c) Freeman, T. L.; Evans, S. D.; Ulman, A. *Langmuir* **1995**, *11*, 4411.

derivatized colloidal silver particles by a simple solution-based immersion procedure. Further, the attractive electrostatic interaction can be modulated by varying the colloidal solution pH thereby altering the degree of ionization of the amine groups in the SAM and carboxylic acid groups on the colloidal particle surface. Silver nanoparticle films on the 4-ATP SAMs of different surface coverage could be obtained using this strategy.

**Acknowledgment.** A.G. thanks the Council for Scientific and Industrial Research (CSIR), Government

of India, for financial support. The authors thank the ESCA group, Special Instruments Laboratory, National Chemical Laboratory, Pune, for assistance with the XPS measurements. This work was supported by a special grant to M.S. from the CSIR.

**Supporting Information Available:** XPS spectra of the Au 4f, Ag 3d, C 1s, and O 1s core levels together with the chemically distinct decomposed components (PDF). This material is available free of charge via the Internet at <http://pubs.acs.org>.

CM990439U